

LETTER • OPEN ACCESS

Climate impact emergence and flood peak synchronization projections in the Ganges, Brahmaputra and Meghna basins under CMIP5 and CMIP6 scenarios

To cite this article: Anne Gädeke *et al* 2022 *Environ. Res. Lett.* **17** 094036

View the [article online](#) for updates and enhancements.

You may also like

- [Increases of extreme heat-humidity days endanger future populations living in China](#)
Huopo Chen, Wenyue He, Jianqi Sun et al.
- [Increasing heat risk in China's urban agglomerations](#)
Guwei Zhang, Gang Zeng, Xin-Zhong Liang et al.
- [Global surface air temperatures in CMIP6: historical performance and future changes](#)
Xuewei Fan, Qingyun Duan, Chenwei Shen et al.



Breath Biopsy® OMNI®

The most advanced, complete solution for global breath biomarker analysis

TRANSFORM YOUR RESEARCH WORKFLOW



Expert Study Design & Management



Robust Breath Collection



Reliable Sample Processing & Analysis



In-depth Data Analysis



Specialist Data Interpretation

ENVIRONMENTAL RESEARCH
LETTERS

LETTER

OPEN ACCESS

RECEIVED
28 January 2022REVISED
15 July 2022ACCEPTED FOR PUBLICATION
25 August 2022PUBLISHED
9 September 2022

Original content from
this work may be used
under the terms of the
[Creative Commons
Attribution 4.0 licence](#).

Any further distribution
of this work must
maintain attribution to
the author(s) and the title
of the work, journal
citation and DOI.

Climate impact emergence and flood peak synchronization
projections in the Ganges, Brahmaputra and Meghna basins
under CMIP5 and CMIP6 scenariosAnne Gädeke^{1,*} , Michel Wortmann^{1,2} , Christoph Menz¹ , AKM Saiful Islam³ ,
Muhammad Masood⁴ , Valentina Krysanova¹ , Stefan Lange¹ and Fred Fokko Hattermann¹ ¹ Potsdam Institute for Climate Impact Research, Member of the Leibniz Association, Telegrafenberg, 14412 Potsdam, Germany² School of Geography and the Environment, University of Oxford, South Parks Road, Oxford OX1 3QY, United Kingdom³ Institute of Water and Flood Management, Bangladesh University of Engineering and Technology, Dhaka 1000, Bangladesh⁴ Bangladesh Water Development Board, Design Circle-9, Pani Bhaban (level-2), 72, Green Road, Dhaka 1215, Bangladesh

* Author to whom any correspondence should be addressed.

E-mail: a.gaedeker@gmail.com**Keywords:** floods, Bangladesh, CMIP6, CMIP5, ISIMIP, time of climate impact emergence, flood peak synchronizationSupplementary material for this article is available [online](#)**Abstract**

The densely populated delta of the three river systems of the Ganges, Brahmaputra and Meghna is highly prone to floods. Potential climate change-related increases in flood intensity are therefore of major societal concern as more than 40 million people live in flood-prone areas in downstream Bangladesh. Here we report on new flood projections using a hydrological model forced by bias-adjusted ensembles of the latest-generation global climate models of CMIP6 (SSP5-8.5/SSP1-2.6) in comparison to CMIP5 (RCP8.5/RCP2.6). Results suggest increases in peak flow magnitude of 36% (16%) on average under SSP5-8.5 (SSP1-2.6), compared to 60% (17%) under RCP8.5 (RCP2.6) by 2070–2099 relative to 1971–2000. Under RCP8.5/SSP5-8.5 (2070–2099), the largest increase in flood risk is projected for the Ganges watershed, where higher flood peaks become the ‘new norm’ as early as mid-2030 implying a relatively short time window for adaptation. In the Brahmaputra and Meghna rivers, the climate impact signal on peak flow emerges after 2070 (CMIP5 and CMIP6 projections). Flood peak synchronization, when annual peak flow occurs simultaneously at (at least) two rivers leading to large flooding events within Bangladesh, show a consistent increase under both projections. While the variability across the ensemble remains high, the increases in flood magnitude are robust in the study basins. Our findings emphasize the need of stringent climate mitigation policies to reduce the climate change impact on peak flows (as presented using SSP1-2.6/RCP2.6) and to subsequently minimize adverse socioeconomic impacts and adaptation costs. Considering Bangladesh’s high overall vulnerability to climate change and its downstream location, synergies between climate change adaptation and mitigation and transboundary cooperation will need to be strengthened to improve overall climate resilience and achieve sustainable development.

1. Introduction

The majority of Bangladesh lies in one of the largest and most populous deltas of the world, downstream of the three river systems of the Ganges, Brahmaputra and Meghna (GBM). Floods are common in the GBM basins and are primarily caused by heavy rain-falls during the summer monsoon season (South/

Southeast Asian monsoon region). Every year, one-quarter to one-third of Bangladesh is inundated (Islam *et al* 2010), impacting approximately 40 million people (>20% of the population) and often leading to a large number of fatalities and human displacements (Mehta and Kumar 2019). Economically, flooding results in large financial losses in the agriculture, housing, industry, and transportation sectors

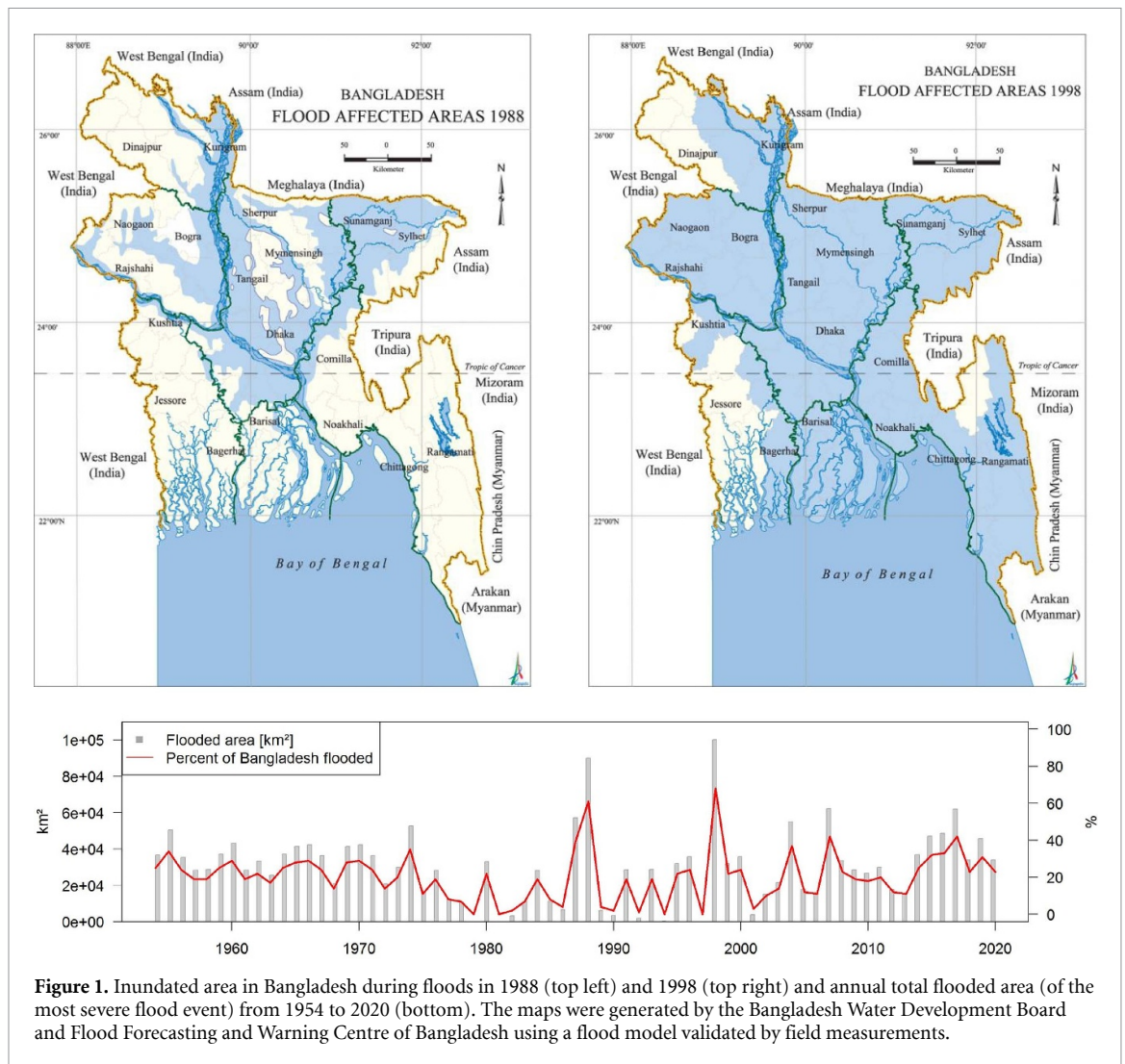


Figure 1. Inundated area in Bangladesh during floods in 1988 (top left) and 1998 (top right) and annual total flooded area (of the most severe flood event) from 1954 to 2020 (bottom). The maps were generated by the Bangladesh Water Development Board and Flood Forecasting and Warning Centre of Bangladesh using a flood model validated by field measurements.

(Mirza 2011). The effects of floods on public health are also a concern, with poor households being particularly vulnerable (Vinke *et al* 2017, Lee *et al* 2021).

Flood duration and recession within Bangladesh depend on the upstream inflow of water, rainfall within Bangladesh, and tidal activity. River floods are particularly severe in Bangladesh if (i) peak flows are of high magnitude and (ii) there is a temporal match of the flood peaks of at least two of the three major rivers. A synchronization of flood peaks at the confluence often results in an increase in flood magnitude and an accelerated flood wave (Guse *et al* 2020). For Bangladesh, flood synchronization has led to catastrophic flood events, such as in 1988 and 1998 (figure 1), when peak flows of the Ganges and Brahmaputra (GB) occurred with a lag of a few days only (Mirza 2002), and the majority of the country was inundated.

Future climate projections based on the Coupled Model Intercomparison Project phase 5 (CMIP5; Taylor *et al* 2012) have indicated increasing air temperature and summer monsoon precipitation over South Asia (Srivastava and DelSole 2014, Uhe *et al* 2019). The evaluation of CMIP5 simulated

precipitation in relation to observations has, however, revealed considerable uncertainties in capturing South Asian summer monsoon onset and precipitation amounts, especially for convective precipitation events (Chen and Zhou 2015, Sabeerali *et al* 2015, Ashfaq *et al* 2017). The latest CMIP6 global climate models (GCMs) differ from those of CMIP5 as a result of improved model parameterization and process representation (Eyring *et al* 2016), a later starting year of the future scenarios (2015 compared to 2006 in CMIP5), updated emission scenarios (shared socioeconomic pathways (SSPs) extending the representative concentration pathways; Meinshausen *et al* 2020), inclusion of new processes (mostly related to atmospheric chemistry and aerosols), higher spatial resolution, and updated land-use scenarios (Gidden *et al* 2019). The starting year of the CMIP6 future projections was updated to 2015 as observational datasets could be extended, especially CO₂ budgets. The 2007–2014 emissions have been notably higher than expected. Therefore the SSP1-2.6 scenario starts, for example, with higher CO₂ concentrations and the emission reductions are more rapid until 2100 compared to RCP2.6. The Indian summer monsoon is

better captured by CMIP6 in comparison to CMIP5 models (Gusain *et al* 2020) as a result of smaller sea surface temperature biases over the Northwestern Pacific Ocean (Xin *et al* 2020). CMIP6 simulations exhibit a larger climate sensitivity to anthropogenic greenhouse gas emissions, which is most likely caused by cloud feedbacks and cloud-aerosol interactions (Meehl *et al* 2020), and resulting in overall higher warming over South Asia (Almazroui *et al* 2020). Similar to CMIP5, the CMIP6 models project an increase in total annual precipitation over South Asia during the twenty-first century (Chen *et al* 2020, Wang *et al* 2020), particularly over the northwestern parts of India, Nepal, Bhutan, and Bangladesh (Almazroui *et al* 2020). The differences between CMIP5 and CMIP6 precipitation and air temperature projections are most pronounced toward the end of the twenty-first century.

Previous studies using hydrological models forced by the simulated meteorological output of CMIP5 GCMs suggest an increase in floods risk, even when limiting global warming to 1.5 °C in accordance with the Paris Agreement (Uhe *et al* 2019). Masood *et al* (2015) showed, using a macroscale hydrological model (H08) forced by five CMIP5 GCMs under a high emission scenario (RCP8.5), that the Meghna basin will experience the highest increase in precipitation (+30%) and runoff (+40%) by the end of the century (2075–2099) compared to 1979–2003. Similarly, Mohammed *et al* (2018) highlighted that under different global warming scenarios (1.5 °C, 2.0 °C, and 4.0 °C), peak flows associated with a return interval of 100 years will increase in the GBM basins (Ganges +27%–54%, Brahmaputra +8%–63%), particularly in the Meghna river (+15%–81%), and especially under high warming (4.0 °C). Studies focusing solely on the Brahmaputra River have also found consistent increases in discharge and high flows when using CMIP5 global (Alam *et al* 2021) and CORDEX regional (Islam *et al* 2017) future climate projections. Using the latest generation of climate models (CMIP6), Hirabayashi *et al* (2021) showed that, globally, CMIP6 based flood projections result in similar flood risk compared to CMIP5. Projected flood risk differences between CMIP5 and CMIP6 climate forcing remain unknown in the GBM basins.

Moving beyond climate change impact assessments focusing on differences over time, the time of climate impact emergence (TCIE) is an important risk management indicator (Hawkins and Sutton 2012). TCIE provides stakeholders and policy makers an estimate of the time left for adaptation planning—or in other words when will an extreme flood today be regarded as the ‘new normal’ in the future. The ‘time of emergence’ concept has mostly been applied to climatic variables such as mean temperature and precipitation (Diffenbaugh and Scherer 2011, Hawkins and Sutton 2012). More recently, the concept was extended to impacts assessing hydrological regime

shifts (Leng *et al* 2016, Muelchi *et al* 2021) and future agricultural risks (Jägermeyr *et al* 2021).

The objective of this paper is to assess how the improvements in simulating summer monsoon precipitation of the latest generation of climate projections (CMIP6) translate into high and peak flows in Bangladesh in comparison to the previous generation of climate projections (CMIP5). The study focuses on three main aspects:

- (a) Flood peak synchronization: To identify if there are changes in the likelihood of simultaneous flooding occurring at least two of the major rivers draining into Bangladesh (Meghna, Ganges, Brahmaputra). This could lead to an increased risk for severe flooding in Bangladesh.
- (b) TCIE: To identify the point in time when projected floods under climate change clearly differ from historical floods. This assessment is critical for risk assessments and planning of adaptation measures.
- (c) Two global warming scenarios (RCP2.6/SSP1-2.6—RCP8.5/SSP5-8.5): To refine our understanding of the effects of stringent climate mitigation policies on flooding in the GBM basins and their consequences for Bangladesh.

2. Overview of study basins

The watersheds of the GBM rivers cover together an area of ~1.6 million km². The Ganges basin (966 000 km²) is the largest, followed by the Brahmaputra (532 000 km²) and the Meghna (80 000 km²). Elevation ranges from sea level to more than 8000 m in the Himalayan Mountains for the Ganges and the Brahmaputra basins and to up to 3000 m in the Manipur Hills for the Meghna basin. The majority of the GBM delta in Bangladesh is less than 12 m above sea level. The GBM basins are shared among five countries: India (64%), China (18%), Nepal (8%), Bangladesh (7%), and Bhutan (3%) (FAO 2011). The individual country share in each basin is detailed in table 1.

The climate is extremely diverse across the GBM basins (FAO 2011). Total annual (summer monsoon season June–September) precipitation amounts are presented in table 1 for the different watersheds. Topography plays a strong role on the spatial distribution of precipitation in the GB watersheds (figure S1). Precipitation is the lowest across the Tibetan Plateau (table 1 (China)) and the upper northwestern region of the Ganges watershed. In the Brahmaputra basin, large precipitation amounts occur across the Himalaya belt and the lowlands. The Meghna watershed receives the largest amount of precipitation per km², with the world’s highest precipitated area (Cherrapunji-Mawsynram region) receiving average annual precipitation of around 12 000 mm in the hilly northeastern state of Meghalaya (India)

Table 1. Overview of hydro-climatic watershed characteristics. The meteorological variables were obtained from the W5E5 dataset (Lange *et al* 2021) covering the period 1979–2019 and are presented as mean and summer (June–September (JJAS)) annual means/sums. Discharge data were obtained from the Bangladesh Water Development Board for the stations Hardinge Bridge (Ganges), Bahadurabad (Brahmaputra) and Bhairab Bazar (Meghna). The number of dams/reservoirs is obtained from Lehner *et al* (2011).

	Precipitation annual/ JJAS (JJAS share (%)) (mm a ⁻¹)	Air temperature annual/JJAS (°C)	Annual maximum (mean) discharge (m ³ s ⁻¹)/(mm)	Dams/Reservoirs (number)
Ganges ^a	1123/939 (84)	21.7/26.2	55 000 (15 701)/	75
India (79%)	1008/877 (87)	24.9/29.0	1800 (510)	74
China (3%)	912/650 (71)	−3.4/4.4		—
Nepal (14%)	1670/1323 (79)	13.4/18.9		1
Bangladesh (4%)	1875/1411 (75)	25.3/28.4		—
Brahmaputra ^a	1533/1062 (69)	9.0/15.1	82 000 (24 027)/	10
India (36%)	2753/1875 (68)	19.7/24.1	4860 (1420)	4
China (50%)	566/409 (72)	0.6/8.1		3
Bangladesh (7%)	2098/1466 (70)	25.5/28.8		1
Bhutan (7%)	1549/1109 (72)	10.8/16.1		—
Meghna ^a	3138/2093 (67)	23.2/26.4	13 000 (5486)/	—
India (57%)	3195/2123 (66)	21.8/24.9	5125 (2160)	—
Bangladesh (43%)	2616/1723 (66)	25.3/28.4		—

^a Basin average.

(Das *et al* 2018). Within Bangladesh, a humid subtropical climate dominates, with mean annual precipitation ranging from 1500 mm in the west to about 4200 mm in the northeastern parts of the country (Shahid 2011, Mohammed *et al* 2018). About 80% of the total annual rainfall occurs in the summer monsoon season (Mirza 2002, Islam *et al* 2010). The remaining precipitation is distributed between the pre-monsoon (March–May) and post-monsoon (October–November) seasons.

The annual maximum (mean) discharge amounts to $\sim 55\,000$ ($\sim 16\,000$) m³ s⁻¹ in the Ganges river at Hardinge Bridge (1980–2012), $\sim 82\,000$ ($\sim 24\,000$) m³ s⁻¹ in the Brahmaputra river at Bahadurabad (1980–2012) and $\sim 13\,000$ (~ 5500) m³ s⁻¹ in the Meghna river at Bhairab Bazar (1984–2012) on average based on discharge data provided by the Bangladesh Water Development Board. For better inter-basin comparison, runoff records (mm) are shown in table 1.

The land use distribution also differs between the watersheds (figure S2). The Indo-Gangetic Plain is largely used for agriculture (‘South Asia’s bread basket’), the Himalaya belt is forested, while savanna and grasslands dominate the Tibetan plateau. Glaciers, located at high altitudes, cover 0.02% of the Ganges and 0.85% of the Brahmaputra basins (RGI 2017). There are no documented glaciers nor permanent snowfields in the Meghna basin due to topographic and climatic conditions. Upstream regions in the Brahmaputra and the Ganges watershed are highly dependent on the seasonal snow and ice-melt for agriculture and hydropower generation (Immerzeel *et al* 2010, Ray *et al* 2015, Biemans *et al* 2019). For Bangladesh, the glacier melt contribution to total discharge is negligible, although glacier melt and extreme monsoon precipitation tend to temporally

coincide. Based on the degree-day approach (which is also used in the hydrological model Soil and Water Integrated Model (SWIM) applied in this study) and upper-range values for the melt parameter, the glacier meltwater contribution to the mean annual maximum discharge (Q_{\max}) was approximately 1.4% ($\sim 0.15\%$ in the Ganges and 2.5% in the Brahmaputra basins) and considerably less for the periods of more severe floods. With a projected glacier recession, this percentage is likely to decrease further in the future (Lutz *et al* 2014).

3. Methods and data

3.1. Data

All data used (table S1) are open data except for the daily discharge. The daily discharge records from the gauging stations within Bangladesh (Hardinge Bridge, Bahadurabad, Bhairab Bazar) were provided by the Bangladesh Water Development Board and cover the period 1980–2012 (Hardinge Bridge, Bahadurabad) and 1984–2012 (Bhairab Bazar) (table S2). Here, we refer to these stations as outlet stations. Monthly discharge data from nine stations located in Nepal, in the upstream parts of the Ganges basin, were obtained from the Global Run-off Data Center (table S1). Table S2 summarizes the discharge data’s location, temporal coverage, and quality.

Observation-based climate data (table S1) was obtained from two datasets: EWEMBI (Lange 2016) and W5E5 version 2 (Lange *et al* 2021). Both datasets are available globally at 0.5° horizontal spatial resolution and at daily time step. The EWEMBI dataset, covers the time period 1979–2013 and W5E5 the period 1979–2019. Data sources of EWEMBI are ERA-Interim reanalysis data (Dee *et al* 2011),

WATCH methodology applied to ERA-Interim reanalysis data (Weedon *et al* 2014), earth2OBServe (E2OBS) forcing data (Calton *et al* 2016) and NASA/GEWEX Surface Radiation Budget data (Stackhouse *et al* 2011). The Surface Radiation Budget data were used to bias-correct E2OBS shortwave and longwave radiation (Lange 2018). W5E5 combines version 2.0 of the WATCH Forcing Data methodology applied to ERA5 data (Weedon *et al* 2014, Cucchi *et al* 2020) over land with ERA5 reanalysis data (Hersbach *et al* 2020) over the ocean. Precipitation over the land is bias-adjusted using observations from the Global Precipitation Climatology Centre (GPCC; Schneider *et al* 2011, version 6) and over the ocean using the Global Precipitation Climatology Project (Adler *et al* 2003, version 2.3).

Meteorological outputs (precipitation, air temperature (mean, minimum, maximum), humidity, downward shortwave radiation) of four CMIP5 and ten CMIP6 GCMs (table S3) were bias-adjusted at daily temporal resolution and statistically downscaled to 0.5° spatial resolution within the Inter-Sectoral Impact Model Intercomparison Project (ISIMIP) phases 2b (for CMIP5) and 3b (for CMIP6). The CMIP5 and CMIP6 GCMs used here were selected by ISIMIP based on benchmark performance during the historical period, equilibrium climate sensitivity, structural independence, output availability at the time of selection, and representation of the entire CMIP ensemble (details see in Frieler *et al* 2017). The bias-adjusted climate models form the basis for impact studies across many different sectors (www.isimip.org/). The ten CMIP6 GCMs were bias-adjusted to the W5E5 dataset, employing a quantile mapping approach that preserves trends in all quantiles of the distribution of simulated daily climate model outputs (Lange 2019). The bias-adjustment of the four CMIP5 models is based on the EWEMBI data set (1979–2013) based on a slightly advanced version of the method by Hempel *et al* (2013) as detailed in Frieler *et al* (2017) and Lange (2017). The approach is based on transfer functions that correct the multi-year monthly mean value followed by an adjustment of the intra-monthly day-to-day variability. This method only preserves long-term mean-value trends in the climate variables. For the sake of brevity, in the following we refer to the bias-adjusted and statistically downscaled climate inputs from ISIMIP as CMIP5 and CMIP6 climate forcing, although our datasets presents only a subset of the available CMIP5/CMIP6 models. The comparison of the long-term mean spatial patterns of total annual and monsoon season precipitation (figure S1) and precipitation climatology (figure S3) shows a good agreement between the observation-based datasets (W5E5, EWEMBI) and CMIP5, CMIP6 and also in comparison to GPCC (table S4).

3.2. Hydrological model, set-up and evaluation

We used the process-based, semi-distributed SWIM (Krysanova *et al* 1998, 2015) to simulate the hydrological cycle of the GBM basins at a daily time step. SWIM was developed based on SWAT'93 (Arnold *et al* 1993) and MATSALU (Krysanova *et al* 1989) and has been applied to basins of similar hydro-climatic conditions (Vetter *et al* 2015, Wortmann *et al* 2018). Table S5 provides an overview of the most relevant hydrological processes for this study and their representation in SWIM. SWIM is based on a three-level spatial disaggregation of the basin (catchment, subbasins, hydrotopes). The hydrotopes within a subbasin were constructed based on common land use, soil type, and elevation contours (300 meters). Data sources for elevation, land use and soils are shown in table S1. Glacier cover is considered based on the Randolph Glacier Inventory (RGI 2017), and glacier thickness was estimated by slope inversion and uniform shear stress of 10^5 Pa (Marshall *et al* 2011). Glacier extent was kept constant throughout the simulation periods as we estimated glacier contributions to floods to be negligible (see section 2). Similarly, the land cover was held constant within SWIM as our focus was on evaluating the climate change impact. Due to lack of data, the operation of reservoirs (75 in the Ganges, 6 in the Brahmaputra) is not included in the model parameterization.

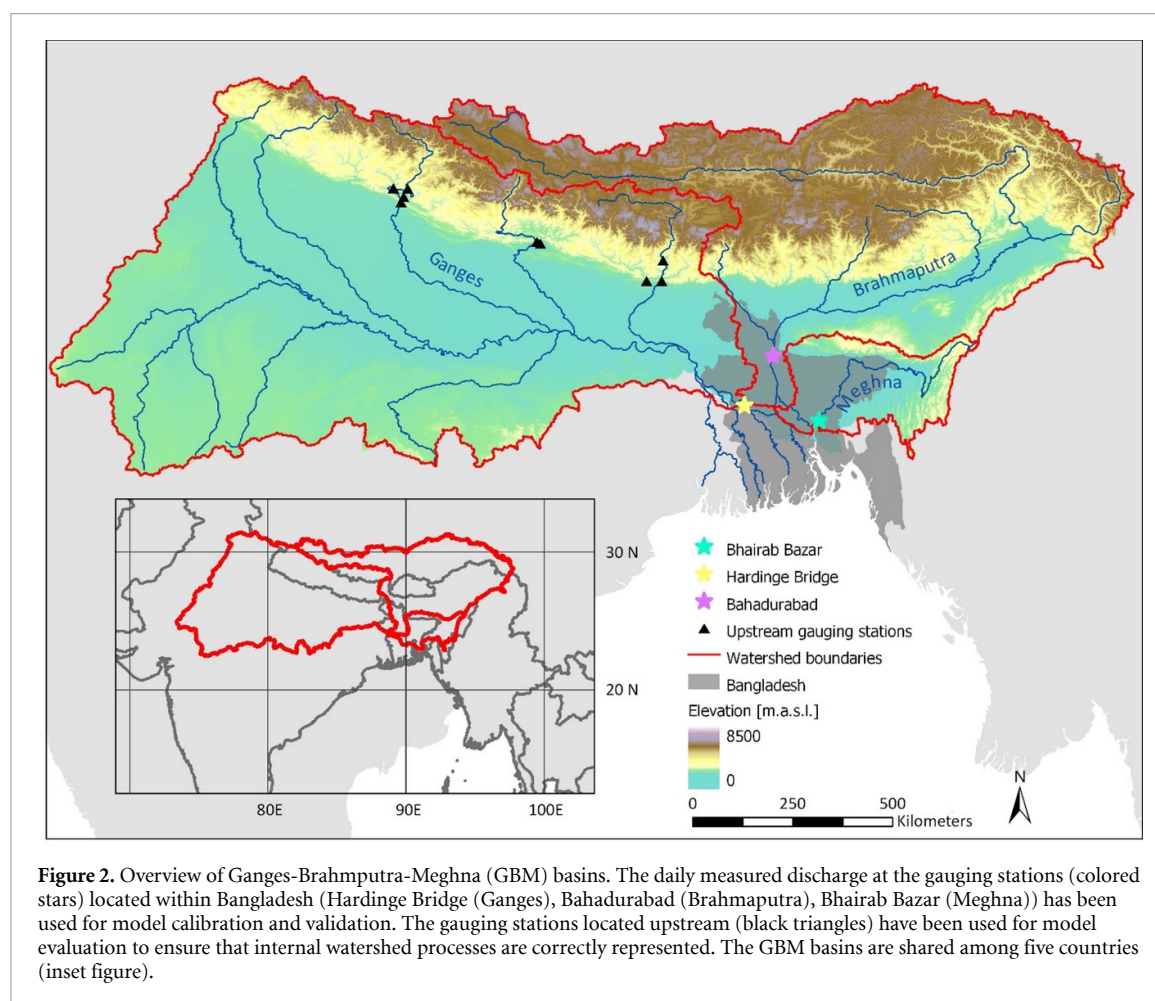
Climate data needed to force SWIM include daily values of minimum, mean and maximum air temperature, total precipitation, solar radiation, and relative humidity. In this study, two SWIM set ups were used:

- EWEMBI-SWIM was calibrated using the meteorological forcing of the observational dataset EWEMBI.
- W5E5-SWIM was calibrated using the meteorological forcing of the observational dataset W5E5.

The calibration (1980–1995) and validation (1996–2012) of SWIM was based, as much as possible, on the enhanced approach by Krysanova *et al* (2018) using multiple statistical performance criteria (table S6). A multi-objective evolutionary algorithm (S-metric selection evolutionary multi-objective optimization algorithm, SMS-EMOA (Beume *et al* 2007)) was used to optimize the SWIM model parameters followed by manual fine-tuning for both model set-ups (EWEMBI and W5E5 climate forcing). The calibrated parameters and their value ranges (used in this study) are displayed in table S9. Calibration on daily discharge was restricted to the outlet stations due to data availability constraints. In the Ganges basin, additional upstream gauging stations, located in Nepal, with monthly discharge records were available for model validation (table S2), which refined the model parameterization to represent internal basin processes reliably.

Table 2. Flood indicators computed for the outlet gauging stations (Bahadurabad (Brahmaputra), Hardinge Bridge (Ganges), Bhairab Bazar (Meghna)).

Indicator	Description
Q_{\max} (a proxy for floods)	Annual maximum (daily mean) discharge ($\text{m}^3 \text{s}^{-1}$)
Q_{10} (a proxy for high flows)	The magnitude of daily discharge that is exceeded 10% of the time in the daily time series of 30 years
$t(Q_{\max})$	Timing of Q_{\max} (day and month)
Flood synchronization	Two criteria need to be fulfilled: (a) Q_{\max} of rivers occurs within 10, 20, 30 days (b) Sum of Q_{\max} must be larger than sum observed $Q_{0.1}$ of rivers ($\Sigma Q_{0.1} = 200\,000 \text{ m}^3 \text{ s}^{-1}$, $185\,000 \text{ m}^3 \text{ s}^{-1}$, $130\,000 \text{ m}^3 \text{ s}^{-1}$, $93\,000 \text{ m}^3 \text{ s}^{-1}$ for GBM, GB, BM, GM, respectively), (Table S7 including periods).
TCIE	Time of climate impact emergence (year)



3.3. Indicators to assess climate change impact

SWIM was forced by the four CMIP5 (using calibrated/validated EWEMBI-SWIM) and ten CMIP6 (using calibrated/validated W5E5-SWIM) climate projections under the RCP2.6/RCP8.5 and SSP1-2.6/SSP5-8.5 scenarios, respectively. The radiative forcing levels of the chosen global warming scenarios are similar for RCP2.6/SSP1-2.6 and RCP8.5/SSP5-8.5 by 2100. The low-end global warming scenarios RCP2.6/SSP1-2.6 present the emission pathways limiting global warming to 2.0 °C above the pre-industrial levels. RCP8.5/SSP5-8.5, on the contrary, represent the high-end global emission scenarios. In

total, the model ensemble consisted of 28 simulations. We defined 1971–2000 to represent the reference period, 2031–2060 the near and 2070–2099 the far future. The impact of climate change on floods in Bangladesh was evaluated using different flood indicators, which are detailed in table 2. The indicators include a proxy for floods (Q_{\max}) and high flows (Q_{10}), timing and synchronization of Q_{\max} and TCIE. Flood indicators were calculated at the outlet discharge stations of the three rivers located in Bangladesh (figure 2). We applied a Wilcoxon rank-sum test to assess the statistical significance of the changes.

We evaluated flood synchronization across the three river basins for each river basin combination (GB, Brahmaputra and Meghna (BM), and Ganges and Meghna (GM), and all three river basins (GBM)) within a time period of 10, 20, and 30 d. We only evaluated events when the combined Q_{\max} of the two or three rivers exceeds a threshold value ($\Sigma Q_{0.1}$), which is based on the discharge magnitude that was exceeded on only 0.1% of all days of the observations ($Q_{0.1}$, table S7). We counted the number of occurrences of such synchronous floods for each model ensemble member within each time period.

We also computed the TCIE following the definition and approach described in Jägermeyr *et al* (2021). TCIE defines the year when the average climate change impact occurs outside the envelope of the historical Q_{\max} flow variability. More specifically, the TCIE is the year in which the 30 year moving-average of simulated Q_{\max} (ensemble median) exceeds either the 95th (positive TCIE) or 5th (negative TCIE) percentile of the simulated Q_{\max} (ensemble median) of the reference period (1971–2000).

4. Results

4.1. Model calibration and validation

The performance of SWIM was evaluated for both mean and high flow conditions. Results are largely similar for the two model versions (EWEMBI-SWIM, W5E5-SWIM). The comparison of daily simulated and measured discharge (figures S4(a), (c) and (e)) at the outlet stations shows high scores of the statistical performance criteria (table 3). Model performance is, on average, slightly lower during the model validation period compared to the calibration period. In the Ganges basin, good model performance was also achieved at most upstream gauges, which indicates that internal watershed processes are captured sufficiently well (figure S5). In the Brahmaputra basin, simulations and observations show higher differences compared to other two basins, which can be directly linked to data availability (no upstream discharge records) to constrain model parameterization. The seasonal discharge cycle is quite well reproduced by the SWIM simulations (figures S4(b), (d) and (f)). Larger differences in simulating seasonality exist based on W5E5 in the Brahmaputra (underestimation especially from July to September) and in the Ganges (overestimation from mid-August to September).

The recurrence intervals of Q_{\max} show a good agreement between observations and SWIM simulations forced by the observation-based datasets (EWEMBI, W5E5) as well as the historical CMIP simulations (figure 3). Difference between SWIM forced

by EWEMBI or W5E5 are minor when assessing daily peak flows. At Hardinge Bridge (Ganges), simulated Q_{\max} by EWEMBI-SWIM (W5E5-SWIM) slightly underestimate (overestimate) the magnitude of frequent high flow events (return period of up to 5 years), low frequency events (return period >5 years) are generally underestimated by the simulations. At Bahadurabad (Brahmaputra), Q_{\max} of high frequency are well captured, while events of lower frequency tend to be underestimated by the simulations. At Bhairab Bazar (Meghna), higher (lower) frequency events are underestimated (well captured). Differences of Q_{\max} recurrence intervals between the CMIP historical climate forcing and the observation-based dataset used for the bias-adjustment, are low, except in the Brahmaputra basin and especially for CMIP5 versus EWEMBI.

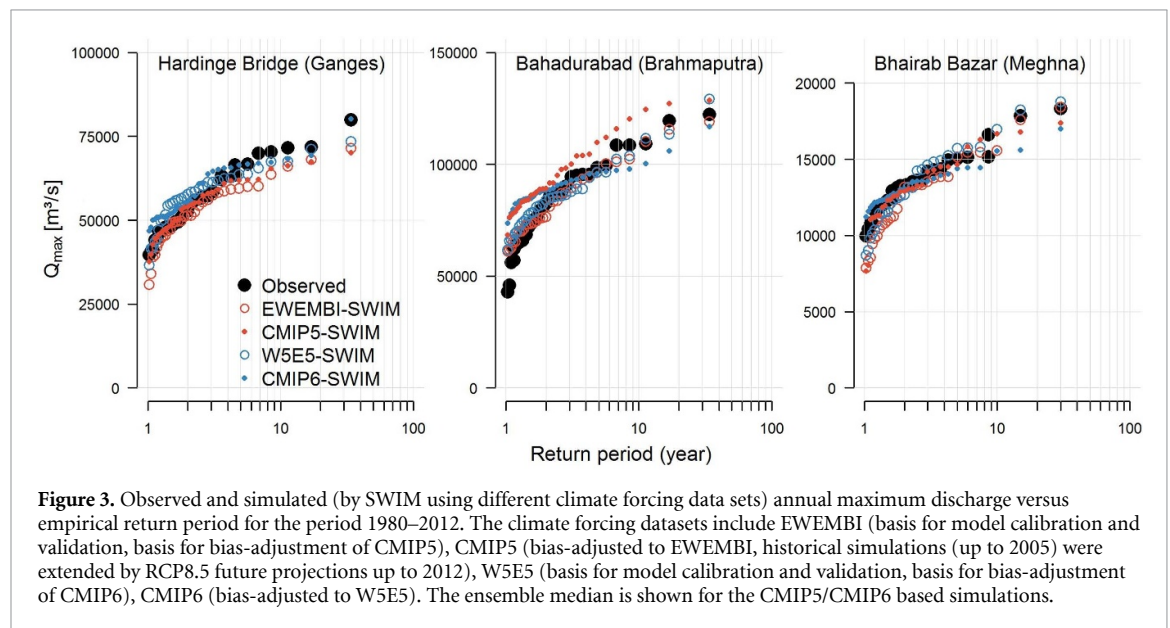
4.2. Climate change impact assessment

The climate model ensembles consistently project increases in median summer monsoon season air temperature and precipitation across the GBM basins and global warming scenarios, despite large variability across the model ensembles (figure 4, table S8). The air temperature increase is largest under RCP8.5/SSP8.5 in the far future, especially in the Brahmaputra basin (>4 °C). The temperature increase is significant ($p < 0.05$) across all scenarios and is comparable between CMIP6 and CMIP5 (table S8). Considering the changes in the multi-model median, stringent climate mitigation policies limit warming to an increase of less than 2 °C (RCP2.6/SSP1-2.6) and summer precipitation increase to less than 10% in the GBM basins (except in the Ganges (CMIP6) and Meghna (CMIP5)). The CMIP5 models simulate the largest increase in summer monsoon season precipitation in the Meghna basin ($28 \pm 13\%$) under RCP8.5 in the far future (ensemble median \pm interquartile range (difference between 75th and 25th percentiles)), while the CMIP6 models simulate the largest increase in the Ganges basin ($27 \pm 22\%$ under SSP5-8.5 in the far future) (table S8).

Under all climate change scenarios, a consistent increase in high flows (Q_{10}) and flood peaks (Q_{\max}) is simulated in the near and far future (figure 4, table S8). The largest percent increase in Q_{10} and Q_{\max} is projected in the Ganges basin under RCP8.5/SSP5-8.5 in the far future. The increase in Q_{10} and Q_{\max} amplifies until the end of the century under RCP8.5/SSP5-8.5, while remaining relatively stable under RCP2.6/SSP1-2.6. Stringent emission reductions even result in a decrease of Q_{\max} under the SSP1-2.6 scenario in the far compared to the near future. In the Meghna watershed, however, Q_{10} and Q_{\max} increase from the near to the

Table 3. Statistical performance criteria during SWIM calibration (1980–1995) and validation (1996–2012) based on daily discharge at the gauging stations Bhairab Bazar (Meghna), Hardinge Bridge (Ganges) and Bahadurabad (Brahmaputra), which are located in Bangladesh prior to their confluence. SWIM was calibrated using meteorological forcing of EWEMBI (basis for bias-adjustment of CMIP5) and W5E5 (basis for bias-adjustment of CMIP6). The statistical performance criteria include: Nash–Sutcliffe efficiency (NSE) (Nash and Sutcliffe 1970), percent bias (PBIAS) (%), mean error (ME) ($\text{m}^3 \text{s}^{-1}$), Coefficient of determination (R^2), Index of Agreement (IoA) and the ratio of standard deviation (rSD).

		NSE	PBIAS	ME	R^2	IoA	rSD	
Climate forcing	<i>Ganges (Hardinge Bridge)</i>							
	EWEMBI	Calibration	0.92	−6.6	821	0.97	0.9	1.10
		Validation	0.84	0.4	−61	0.92	0.85	1.03
	W5E5	Calibration	0.86	11.5	−1423	0.93	0.86	0.98
		Validation	0.83	18.4	−3129	0.93	0.84	0.93
	<i>Brahmaputra (Bahadurabad)</i>							
EWEMBI	Calibration	0.85	−7.7	1727	0.93	0.79	0.80	
	Validation	0.77	−5.4	1334	0.88	0.77	0.91	
W5E5	Calibration	0.69	−16.1	3593	0.86	0.75	0.99	
	Validation	0.52	−17	4210	0.82	0.71	1.13	
<i>Meghna (Bhairab Bazar)</i>								
EWEMBI	Calibration	0.91	−2.2	112	0.96	0.87	1.05	
	Validation	0.85	−11.2	612	0.95	0.84	1.09	
W5E5	Calibration	0.87	4.3	−222	0.94	0.85	0.98	
	Validation	0.85	−4.9	267	0.93	0.84	1.03	



far future under the RCP2.6. When comparing the CMIP phases, a strong increase in Q_{\max} (ensemble median) of 60% is projected under RCP8.5, compared to 36% under SSP5-8.5 in the far future relative to the reference when averaged across the GBM basins (weighted by basin area). For Q_{10} , the increase is comparable between the CMIP phases (RCP8.5: 42%, SSP5-8.5: 44%). Comparing the CMIP5 and CMIP6 forcing for the separate basins shows that: In the BM basins, percent increase in Q_{10} and Q_{\max} is

larger for CMIP5 compared to CMIP6 based projections across all scenarios and periods (except precipitation (RCP2.6, near future) and Q_{10} (RCP8.5, far future) in the Brahmaputra). In the Ganges basin, the percent increase of Q_{10} is larger under CMIP6 across all scenarios and periods, while CMIP5 based simulations result in larger Q_{\max} (except for SSP5-8.5 in the near future).

In the reference period, Q_{\max} (ensemble median) occurs first in the Brahmaputra (late July), followed

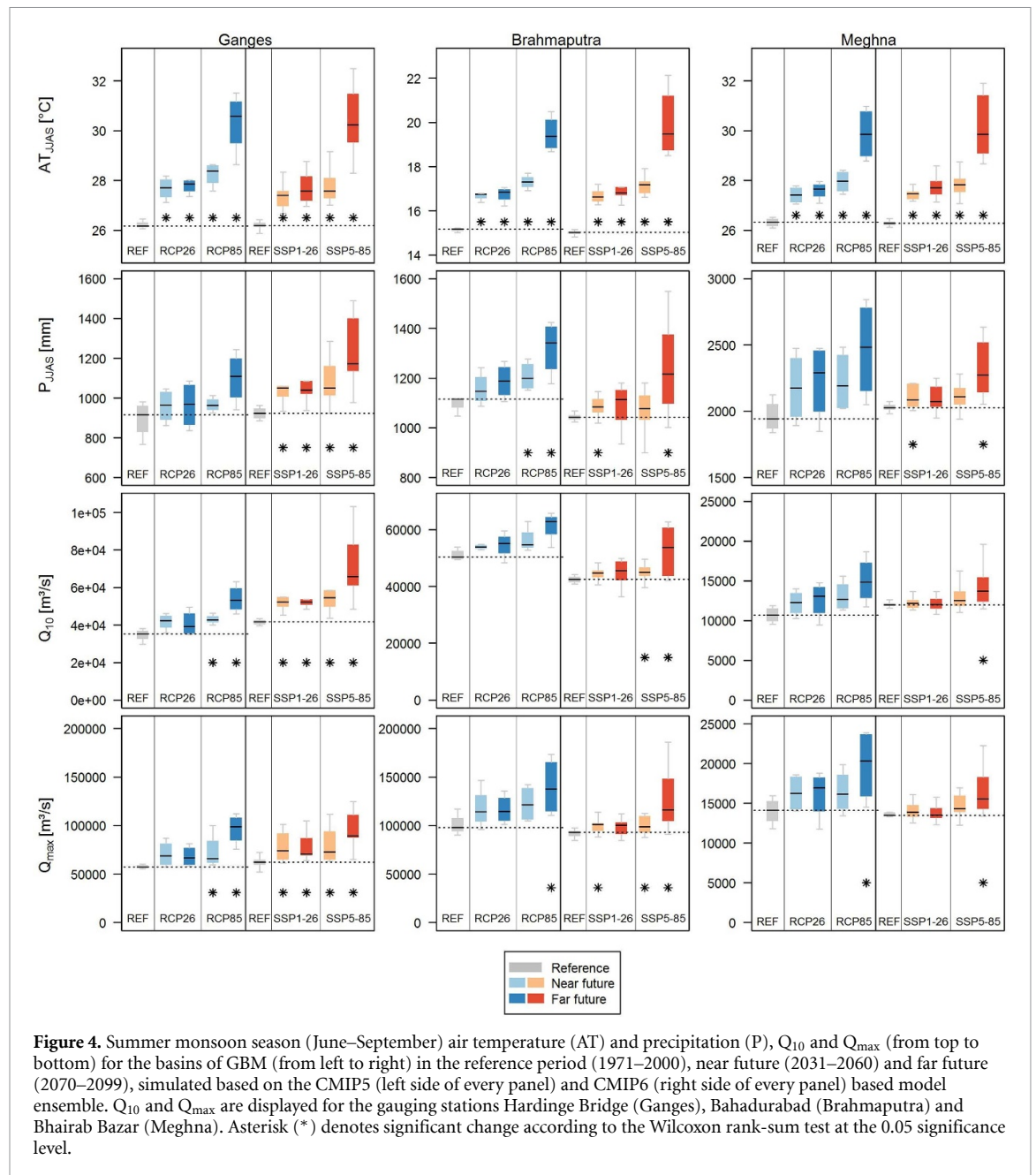


Figure 4. Summer monsoon season (June–September) air temperature (AT) and precipitation (P), Q_{10} and Q_{max} (from top to bottom) for the basins of GBM (from left to right) in the reference period (1971–2000), near future (2031–2060) and far future (2070–2099), simulated based on the CMIP5 (left side of every panel) and CMIP6 (right side of every panel) based model ensemble. Q_{10} and Q_{max} are displayed for the gauging stations Hardinge Bridge (Ganges), Bahadurabad (Brahmaputra) and Bhairab Bazar (Meghna). Asterisk (*) denotes significant change according to the Wilcoxon rank-sum test at the 0.05 significance level.

by the Meghna (mid to late August) and Ganges (late August to early September) rivers (figure 5). Q_{10} also occurs first (late-July) in the Brahmaputra river, and at similar time (late July to early August) at the GM rivers (figure S7, reference period). In all basins, Q_{max} occurs earlier under CMIP5 compared to CMIP6 simulations ($\sim 1\text{--}2$ weeks) in the reference period. In the Ganges basin, the timing of Q_{max} occurrence remains unchanged under the future projections (compared to the reference) under CMIP6, while for CMIP5 Q_{max} occurs later (earlier) under RCP2.6 (RCP8.5). For the Brahmaputra river, a tendency toward earlier occurrence of Q_{max} (more pronounced under CMIP5 compared to CMIP6) is

simulated when considering the ensemble median under all future scenarios, except in the near-future under the CMIP6 SSP scenarios. In the Meghna river, Q_{max} occurs earlier in the near future and later in the far future under CMIP6 future projections compared to the reference. Under CMIP5, there is tendency towards earlier occurrence of Q_{max} , except under RCP8.5 in the near future when no change compared to the reference is simulated. Q_{10} occurs consistently earlier across all scenarios and in all river basins (figure S7).

The likelihood of simultaneously occurring Q_{max} (ensemble median) at the confluence of the rivers increases under all scenarios when considering all

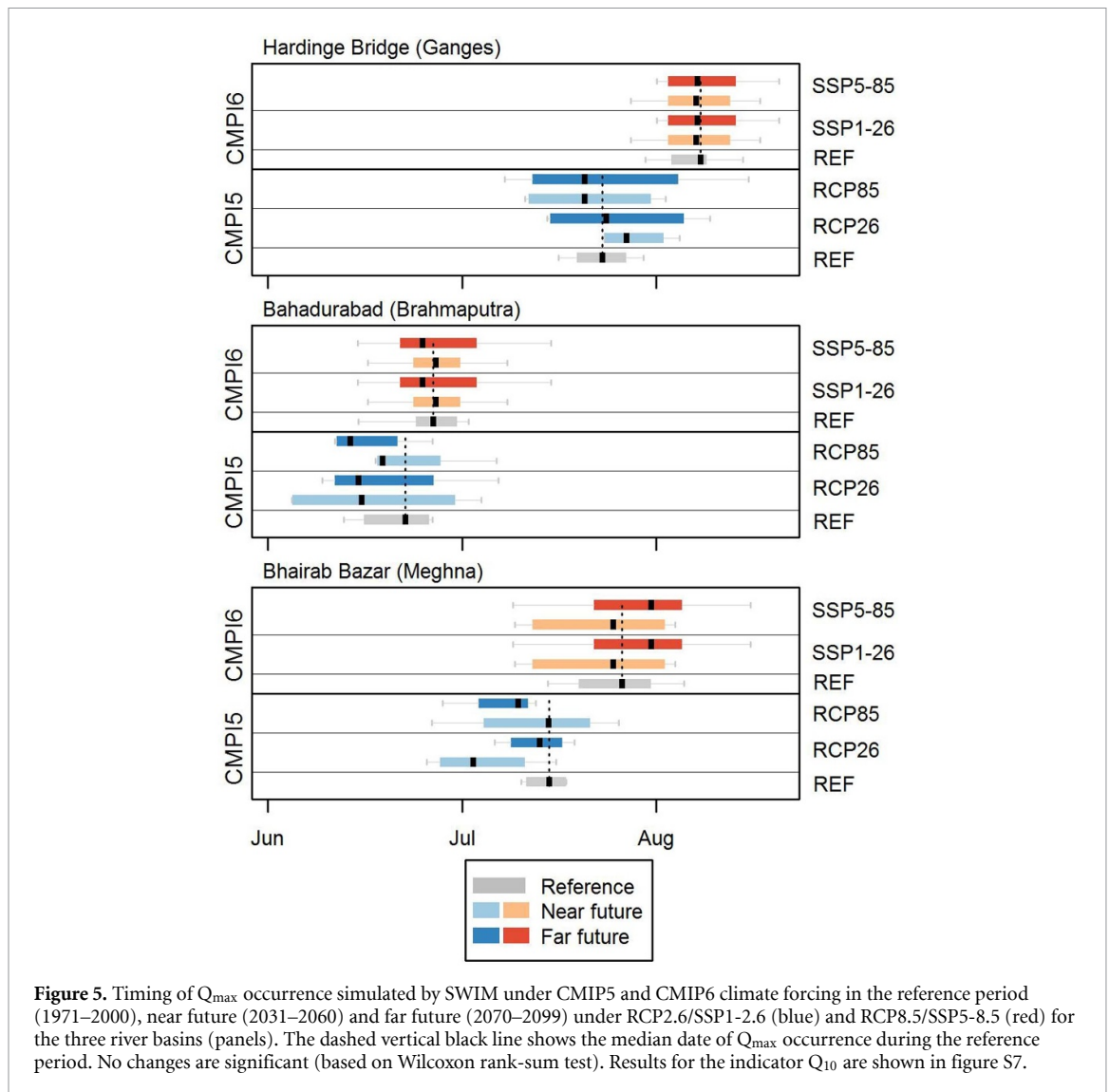
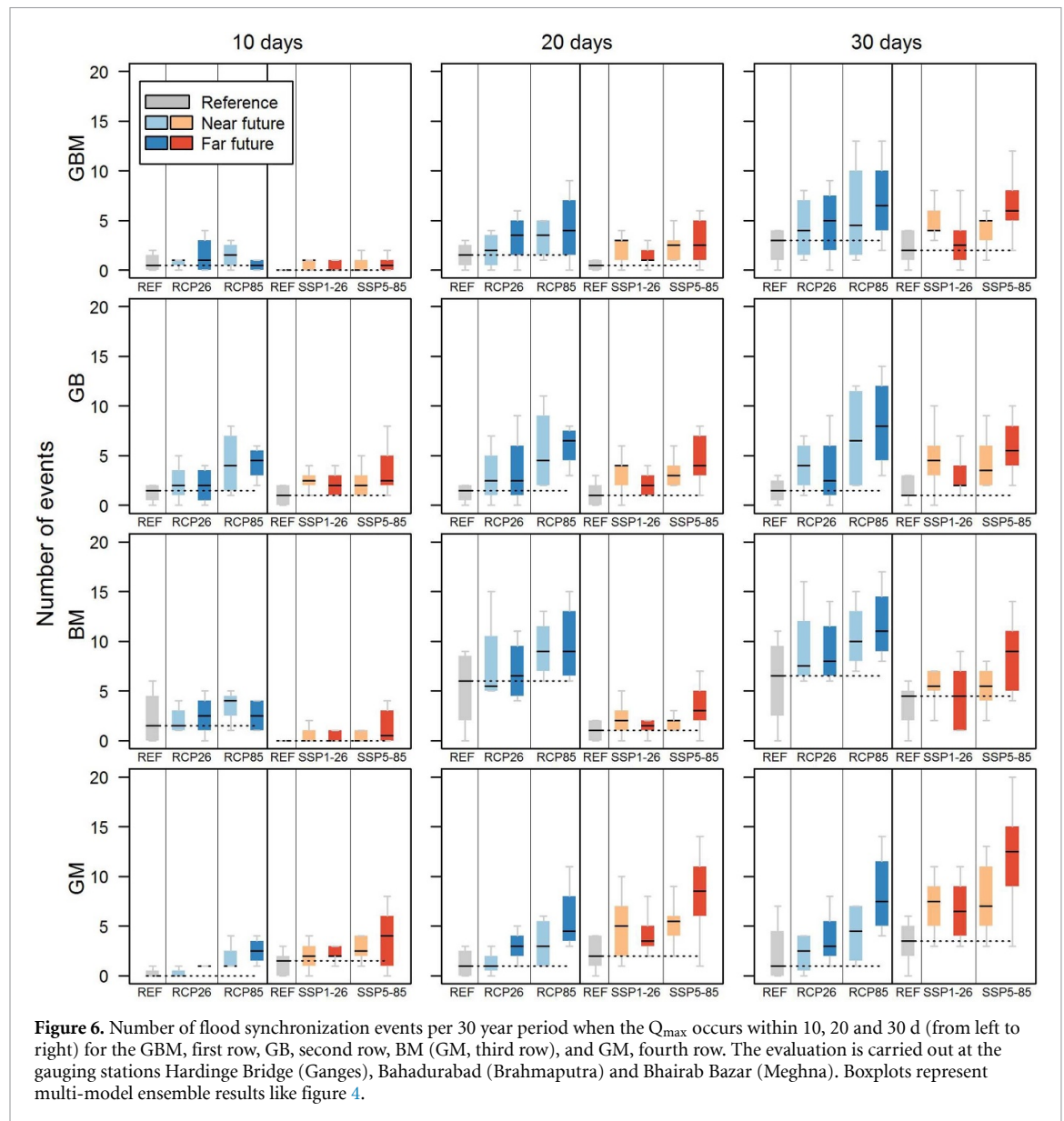


Figure 5. Timing of Q_{max} occurrence simulated by SWIM under CMIP5 and CMIP6 climate forcing in the reference period (1971–2000), near future (2031–2060) and far future (2070–2099) under RCP2.6/SSP1-2.6 (blue) and RCP8.5/SSP5-8.5 (red) for the three river basins (panels). The dashed vertical black line shows the median date of Q_{max} occurrence during the reference period. No changes are significant (based on Wilcoxon rank-sum test). Results for the indicator Q_{10} are shown in figure S7.

three rivers, except in three combinations (10 d, SSP5-8.5 near future, SSP1-2.6 and RCP8.5 far future, figure 6) when no change is simulated. Such events have a magnitude of at least $200\,000\text{ m}^3\text{ s}^{-1}$ and occur between zero (10 d window) to six times (30 d window) within a 30 year period under RCP8.5/SSP5-8.5 (ensemble median). The likelihood of simultaneously occurring Q_{max} from two out of three river systems increases in most scenarios (89 out of 96 combinations (rivers, ensemble, scenario)). Exceptions are a decrease only for Brahmaputra-Meghna in the near future relative to the reference when forced by RCP2.6 (CMIP5). For all river combinations, higher chances of synchronized Q_{max} is simulated during the reference period when SWIM is forced by CMIP5 climate data except for the combination Ganges-Meghna. Projections under CMIP5 RCP8.5 forcing show more frequently occurring simultaneous Q_{max} for all combinations except Ganges-Meghna relative to CMIP6 SSP5-8.5 forcing.

The TCIE is positive, which means that the simulated 30 year moving average of Q_{max} (ensemble median) exceeds historical Q_{max} variability (expressed by the 95th percentile) of the reference period (1971–2000), in all basins until 2100 (figure 7). In the Ganges basin, TCIE occurs between the years 2034 and 2042 (all scenarios), which is considerably earlier compared to the other basins. TCIE is comparable between CMIP5 and CMIP6 based projections in the Ganges. The main difference between the CMIP phases is that under the SSP1-2.6 scenario, the simulated 30 year moving average of Q_{max} remains outside of the envelope of the historic Q_{max} variability after 2040, while under RCP2.6, mitigation efforts result in returning to the historical Q_{max} flow variability after ~ 2060 . Projections show positive TCIE after the year 2070 in the BM basins under the scenarios SSP5-8.5/RCP8.5, ranging between 2073 (CMIP5) and 2078 (CMIP6) in the Brahmaputra and between 2073 (CMIP5) and 2095 (CMIP6) in



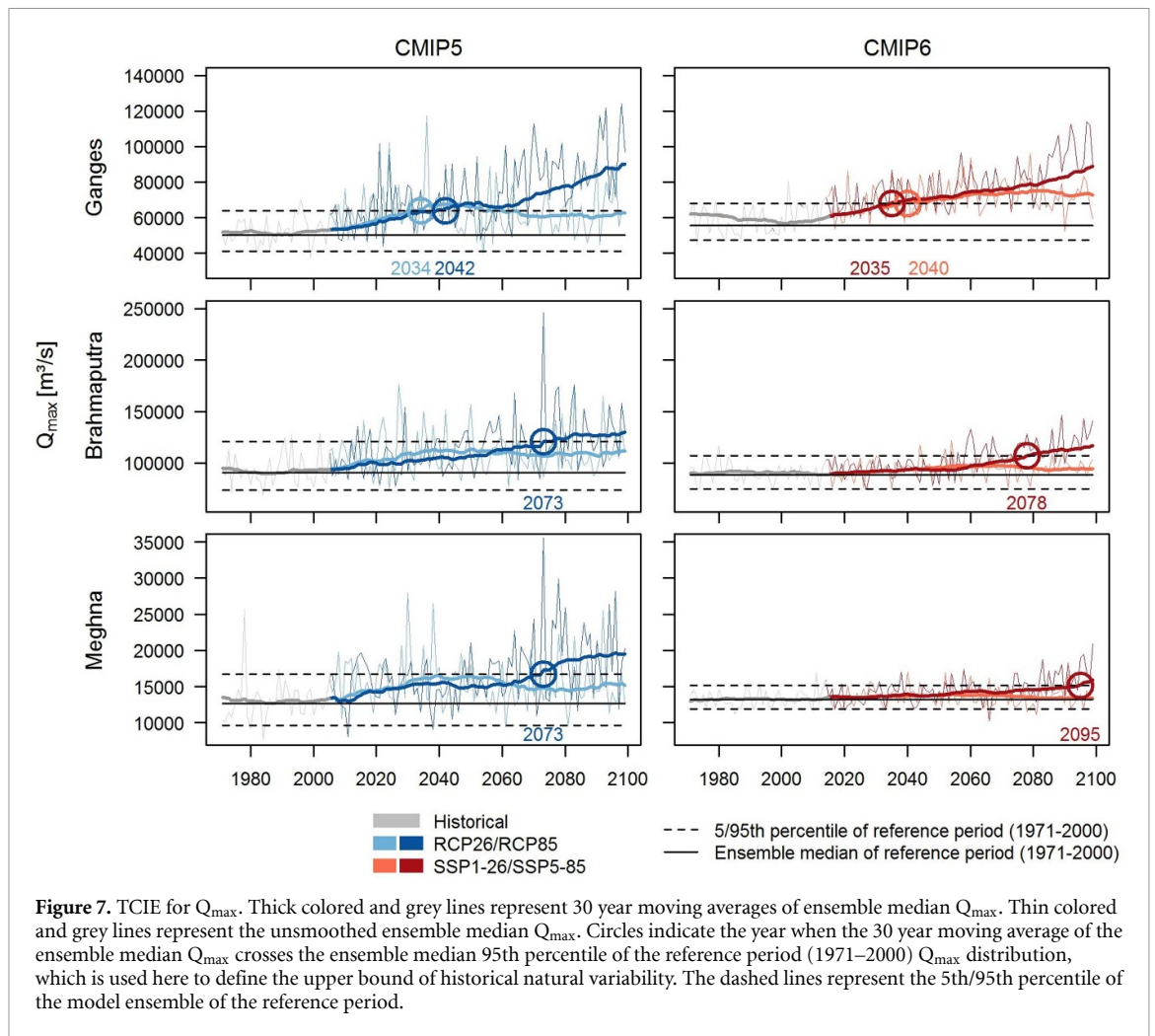
the Meghna basin. This implies that the TCIE occurs earlier (5 years the Brahmaputra, 22 years Meghna) under CMIP5 compared to CMIP6 forcing. Q_{\max} stays below the 95th percentile threshold (and therefore within the envelope of the reference Q_{\max} variability) under RCP2.6/SSP1-2.6 in the BM rivers.

5. Discussion and conclusion

Our flood simulations for the Ganges-Brahmaputra-Meghna basins using the latest climate projections (CMIP6) indicate increases in high flows (Q_{10}) and floods (Q_{\max}) in the 21st century, which is in line with previous estimates based on CMIP5 (Masood and Takeuchi 2015, Mohammed *et al* 2018, Uhe *et al* 2019). The projections show consistently that the Ganges basin is most prone to increased flooding, both in terms of magnitude and TCIE, under future climate change. In the BM basins, projections for high

flows and floods are consistently lower (magnitude and TCEI) based on CMIP6 compared to CMIP5 scenarios. In the Meghna basin, the differences are most pronounced (e.g. TCEI occurs 20 years earlier under CMIP5 versus CMIP6 projections). While the overall variability across the ensemble remains high, our findings suggest robust increases in flood characteristics in the GBM basins.

High flow (Q_{10}) and flood (Q_{\max}) projections under RCP2.6/SSP1-2.6 and RCP8.5/SSP5-8.5 are largely similar up to the middle of the century (~ 2050), suggesting that climate mitigation efforts will only become effective in the second half of the century. Stringent climate mitigation policies have the potential to limit the climate impact on floods to within the envelope of historical variability, as suggested by our TCIE analysis (figure 7). This would considerably reduce adaptation costs. Continuing high greenhouse gas emissions will result in considerable



increases in high flows and floods in the second part of the century. The TCIE analysis highlights that major shifts in flooding due to climate change are projected to occur after 2070 in the BM basins but likely as early as ~ 2040 in the Ganges basin under RCP8.5/SSP5-8.5. The strong increase in high flows and floods under RCP8.5/SSP5-8.5 will translate into increased flood risk and likely devastating socio-economic impacts. Our results indicate that existing flood-protection measures and infrastructure may not be effective and/or sufficient in the future, and that adaptations are needed already in the near future.

Despite the robust signal of increasing floods under climate change, we acknowledge that our approach neglects the uncertainties associated with the hydrological model, as only one hydrological model was used. However, most studies agree that the largest share of uncertainty in climate change impact assessments on water resources stems from the forcing climate models (Gädeke *et al* 2014, Hattermann *et al* 2018) and projecting summer monsoon season precipitation is particularly challenging (Lee *et al* 2018). In addition, our hydrological model setup could be refined by additionally considering climate-induced changes in glacierized areas

(kept constant in our setup) and water management/regulation measures, such as water withdrawals, retention, and storage which play a role in the Ganges basin. However, as floods are primarily caused by (summer) monsoon precipitation and cyclone events in the GBM basins (e.g. Lutz *et al* 2014), glacier melt only plays a minor role during extreme events. Water management/regulation measures are not included due to unavailability of observations/lack of data but are also expected to only play a minor role during extreme flooding. Mohammed *et al* (2018) have pointed out that most water management and regulation measures are designed to be used for water storage rather than flood protection. For example, the Farakka barrage, located in India about 18 km upstream of the border to Bangladesh, diverts water during the dry season and is kept open during the monsoon season to avoid flooding in India.

The climate forcing data poses another uncertainty source. We used the meteorological output of the EWEMBI and W5E5 datasets during the calibration and validation of SWIM. The EWEMBI dataset also served as a basis for bias-adjusting the CMIP5 forcing, while W5E5 was used for bias-adjusting the CMIP6 forcing. In the GM basins, the differences

in Q_{\max} based on CMIP5-SWIM and CMIP6-SWIM forcings are small, while larger differences exist in the Brahmaputra basin (figures 3 and S6). The bias-adjustment and downscaling method used also introduces differences between the CMIP generations. For CMIP6, the improved bias-adjustment and the enhanced downscaling method were found to result in better representation of extreme events and spatial variability (Lange 2019), compared to the approach used for the CMIP5 climate data.

In conclusion, our study provides flood projections using the newest generation of climate projections bias-adjusted for impact assessments. Our results stress the need for considering a potential increase in high flows (up to +44%) and floods (up to +60%) from the three major rivers draining to Bangladesh as well as an increased risk of flood peak synchronization when adapting water management measures in Bangladesh and its upstream neighbors. High emission scenarios suggest a change in flood regimes as early as 2030 in the Ganges implying that flood management will face fundamentally changed risk profiles. This will require substantial investments and, ideally, transparent transboundary coordination of flood risk management considering climate change impacts. The results also indicate how important it is to mitigate climate change and what can be gained when following ambitious reduction targets, whereas failing in this task will imply devastating effects on one of the world's most vulnerable region to climate change in the world.

Data availability statement

All data that support the findings of this study are included within the article (and any supplementary files).

Acknowledgments

This research was carried out in the project 'Oasis Platform for Climate and Catastrophe Risk Assessment—Asia' (18_II_165_Asia_A_Climate and Catastrophe Risk Assessment) funded by the German Federal Ministry for the Environment, Nature Conservation and Nuclear Safety (BMU) as part of the International Climate Initiative (IKI). SL has received funding from the German Federal Ministry of Education and Research (BMBF) under the research QUIDIC (01LP1907A). We thank Dr. Ina Pohle for her valuable feedback.

ORCID iDs

Anne Gädeke  <https://orcid.org/0000-0003-0514-2908>


Michel Wortmann  <https://orcid.org/0000-0002-1879-7674>

Christoph Menz  <https://orcid.org/0000-0001-5127-1554>

AKM Saiful Islam  <https://orcid.org/0000-0002-2435-8280>

Muhammad Masood  <https://orcid.org/0000-0002-4627-1784>

Valentina Krysanova  <https://orcid.org/0000-0002-9481-0148>

Stefan Lange  <https://orcid.org/0000-0003-2102-8873>

Fred Fokko Hattermann  <https://orcid.org/0000-0002-6046-4670>

References

- Adler R F et al 2003 The Version-2 global precipitation climatology project (GPCP) monthly precipitation analysis *J. Hydrometeorol.* **4** 1147–67
- Alam S, Ali M M, Rahaman A Z and Islam Z 2021 Multi-model ensemble projection of mean and extreme streamflow of Brahmaputra River Basin under the impact of climate change *J. Water Clim. Change* **12** 2026–44
- Almazroui M, Saeed S, Saeed F, Islam M N and Ismail M 2020 Projections of precipitation and temperature over the South Asian Countries in CMIP6 *Earth Syst. Environ.* **4** 297–320
- Arnold J G, Allen P M and Bernhardt G 1993 A comprehensive surface-groundwater flow model *J. Hydrol.* **142** 47–69
- Ashfaq M, Rastogi D, Mei R, Touma D and Ruby Leung L 2017 Sources of errors in the simulation of south Asian summer monsoon in the CMIP5 GCMs *Clim. Dyn.* **49** 193–223
- Beume N, Naujoks B and Emmerich M 2007 SMS-EMOA: multiobjective selection based on dominated hypervolume *Eur. J. Oper. Res.* **181** 1653–69
- Biemans H et al 2019 Importance of snow and glacier meltwater for agriculture on the Indo-Gangetic Plain *Nat. Sustain.* **2** 594–601
- Calton B, Schellekens J and Martinez-de L T A 2016 Water resource reanalysis v1: data access and model verification results (version V1.02) (Zenodo) (<https://doi.org/10.5281/zenodo.57760>)
- Chen X and Zhou T 2015 Distinct effects of global mean warming and regional sea surface warming pattern on projected uncertainty in the South Asian summer monsoon *Geophys. Res. Lett.* **42** 9433–9
- Chen Z, Zhou T, Zhang L, Chen X, Zhang W and Jiang J 2020 Global land monsoon precipitation changes in CMIP6 projections *Geophys. Res. Lett.* **47** e2019GL086902
- Cucchi M, Weedon G P, Amici A, Bellouin N, Lange S, Müller Schmied H, Hersbach H and Buontempo C 2020 WFDE5: bias-adjusted ERA5 reanalysis data for impact studies *Earth Syst. Sci. Data* **12** 2097–120
- Das P, Behera M D and Roy P S 2018 Modeling precipitation dependent forest resilience in India *Int. Arch. Photogramm. Remote Sens. Spat. Inf. Sci.* **XLII-3** 263–6
- Dee D P et al 2011 The ERA-Interim reanalysis: configuration and performance of the data assimilation system *Q. J. R. Meteorol. Soc.* **137** 553–97
- Diffenbaugh N S and Scherer M 2011 Observational and model evidence of global emergence of permanent, unprecedented heat in the 20th and 21st centuries *Clim. Change* **107** 615–24
- Eyring V, Bony S, Meehl G A, Senior C A, Stevens B, Stouffer R J and Taylor K E 2016 Overview of the coupled model intercomparison project phase 6 (CMIP6) experimental design and organization *Geosci. Model. Dev.* **9** 1937–58
- FAO 2011 *AQUASTAT Transboundary River Basins—Ganges-BrahmaputraMeghna River Basin* (Rome: Food and Agriculture Organization of the United Nations (FAO))

- Frieler K *et al* 2017 Assessing the impacts of 1.5 °C global warming—simulation protocol of the inter-sectoral impact model intercomparison project (ISIMIP2b) *Geosci. Model. Dev.* **10** 4321–45
- Gädeke A, Hölzel H, Koch H, Pohle I and Grünewald U 2014 Analysis of uncertainties in the hydrological response of a model-based climate change impact assessment in a subcatchment of the Spree River, Germany *Hydrol. Process.* **28** 3978–98
- Gidden M J *et al* 2019 Global emissions pathways under different socioeconomic scenarios for use in CMIP6: a dataset of harmonized emissions trajectories through the end of the century *Geosci. Model. Dev.* **12** 1443–75
- Gusain A, Ghosh S and Karmakar S 2020 Added value of CMIP6 over CMIP5 models in simulating Indian summer monsoon rainfall *Atmos. Res.* **232** 104680
- Guse B, Merz B, Wietzke L, Ullrich S, Viglione A and Vorogushyn S 2020 The role of flood wave superposition in the severity of large floods *Hydrol. Earth Syst. Sci.* **24** 1633–48
- Hattermann F F *et al* 2018 Sources of uncertainty in hydrological climate impact assessment: a cross-scale study *Environ. Res. Lett.* **13** 015006
- Hawkins E and Sutton R 2012 Time of emergence of climate signals *Geophys. Res. Lett.* **39**
- Hempel S, Frieler K, Warszawski L, Schewe J and Piontek F 2013 A trend-preserving bias correction—the ISI-MIP approach *Earth Syst. Dyn.* **4** 219–36
- Hersbach H *et al* 2020 The ERA5 global reanalysis *Q. J. R. Meteorol. Soc.* **146** 1999–2049
- Hirabayashi Y, Tanoue M, Sasaki O, Zhou X and Yamazaki D 2021 Global exposure to flooding from the new CMIP6 climate model projections *Sci. Rep.* **11** 3740
- Immerzeel W W, van Beek L P H and Bierkens M F P 2010 Climate change will affect the Asian water towers *Science* **328** 1382–5
- Islam A K M S, Paul S, Mohammed K, Billah M, Fahad M G R, Hasan M A, Islam G M T and Bala S K 2017 Hydrological response to climate change of the Brahmaputra basin using CMIP5 general circulation model ensemble *J. Water Clim. Change* **9** 434–48
- Islam A S, Haque A and Bala S K 2010 Hydrologic characteristics of floods in Ganges–Brahmaputra–Meghna (GBM) delta *Nat. Hazards* **54** 797–811
- Jägermeyr J *et al* 2021 Climate impacts on global agriculture emerge earlier in new generation of climate and crop models *Nat. Food* **2** 873–85
- Krysanova V, Donnelly C, Gelfan A, Gerten D, Arheimer B, Hattermann F and Kundzewicz Z W 2018 How the performance of hydrological models relates to credibility of projections under climate change *Hydrol. Sci. J.* **63** 696–720
- Krysanova V, Hattermann F, Huang S, Hesse C, Vetter T, Liersch S, Koch H and Kundzewicz Z W 2015 Modelling climate and land-use change impacts with SWIM: lessons learnt from multiple applications *Hydrol. Sci. J.* **60** 606–35
- Krysanova V, Meiner A, Roosaare J and Vasilyev A 1989 Simulation modelling of the coastal waters pollution from agricultural watershed *Ecol. Modelling* **49** 7–29
- Krysanova V, Müller-Wohlfeil D-I and Becker A 1998 Development and test of a spatially distributed hydrological/water quality model for mesoscale watersheds *Ecol. Modell.* **106** 261–89
- Lange S 2016 *EartH2Observe, WFDEI and ERA-Interim data Merged and Bias-corrected for ISIMIP (EWEMBI)* (GFZ Data Services) (<https://doi.org/10.5880/pik.2016.004>)
- Lange S 2017 ISIMIP2b bias-correction code (Zenodo) (<https://doi.org/10.5281/zenodo.1069050>)
- Lange S 2018 Bias correction of surface downwelling longwave and shortwave radiation for the EWEMBI dataset *Earth Syst. Dyn.* **9** 627–45
- Lange S 2019 Trend-preserving bias adjustment and statistical downscaling with ISIMIP3BASD (v1.0) *Geosci. Model. Dev.* **12** 3055–70
- Lange S *et al* 2021 WFDE5 over land merged with ERA5 over the ocean (W5E5 v2.0) *ISIMIP Repository* (<https://doi.org/10.5880/pik.2019.023>)
- Lee D, Ahmadul H, Patz J and Block P 2021 Predicting social and health vulnerability to floods in Bangladesh *Nat. Hazards Earth Syst. Sci.* **21** 1807–23
- Lee D, Min S-K, Fischer E, Shiogama H, Bethke I, Lierhammer L and Scinocca J F 2018 Impacts of half a degree additional warming on the Asian summer monsoon rainfall characteristics *Environ. Res. Lett.* **13** 044033
- Lehner B *et al* 2011 Global reservoir and dam database, Version 1 (Grandv1): Dams, Revision 01 (Palisades: NASA Socioeconomic Data and Applications Center (SEDAC))
- Leng G, Huang M, Voisin N, Zhang X, Asrar G R and Leung L R 2016 Emergence of new hydrologic regimes of surface water resources in the conterminous United States under future warming *Environ. Res. Lett.* **11** 114003
- Lutz A F, Immerzeel W W, Shrestha A B and Bierkens M F P 2014 Consistent increase in high Asia's runoff due to increasing glacier melt and precipitation *Nat. Clim. Change* **4** 587–92
- Marshall S J, White E C, Demuth M N, Bolch T, Wheatle R, Menounos B, Beedle M J and Shea J M 2011 Glacier water resources on the eastern slopes of the Canadian Rocky Mountains *Can. Water Resour. J.* **36** 109–34
- Masood M and Takeuchi K 2015 Climate change impact on the manageability of floods and droughts of the Ganges-Brahmaputra-Meghna basins using flood duration curves and drought duration curves *J. Disaster Res.* **10** 991–1000
- Masood M, Yeh P J-F, Hanasaki N and Takeuchi K 2015 Model study of the impacts of future climate change on the hydrology of Ganges–Brahmaputra–Meghna basin *Hydrol. Earth Syst. Sci.* **19** 747–70
- Meehl G A, Senior C A, Eyring V, Flato G, Lamarque J-F, Stouffer R J, Taylor K E and Schlund M 2020 Context for interpreting equilibrium climate sensitivity and transient climate response from the CMIP6 Earth system models *Sci. Adv.* **6** eaba1981
- Mehta S and Kumar V 2019 Perils of climate change in the Bay of Bengal: India–Bangladesh in perspective *J. Indian Ocean Reg.* **15** 363–72
- Meinshausen M *et al* 2020 The shared socio-economic pathway (SSP) greenhouse gas concentrations and their extensions to 2500 *Geosci. Model. Dev.* **13** 3571–605
- Mirza M M Q 2002 Global warming and changes in the probability of occurrence of floods in Bangladesh and implications *Glob. Environ. Change* **12** 127–38
- Mirza M M Q 2011 Climate change, flooding in South Asia and implications *Reg. Environ. Change* **11** 95–107
- Mohammed K, Islam A K M S, Islam G M T, Alfieri L, Khan M J U, Bala S K and Das M K 2018 Future floods in Bangladesh under 1.5 °C, 2 °C, and 4 °C global warming scenarios *J. Hydrol. Eng.* **23** 04018050
- Muelchi R, Rössler O, Schwanbeck J, Weingartner R and Martius O 2021 River runoff in Switzerland in a changing climate—runoff regime changes and their time of emergence *Hydrol. Earth Syst. Sci.* **25** 3071–86
- Nash J E and J V Sutcliffe 1970 River flow forecasting through conceptual models part I — A discussion of principles *J. Hydrol.*, **10** 282–90
- Ray P A, Yang Y-C E, Wi S, Khalil A, Chatikavanij V and Brown C 2015 Room for improvement: hydroclimatic challenges to poverty-reducing development of the Brahmaputra River basin *Environ. Sci. Policy* **54** 64–80
- RGI 2017 Randolph glacier inventory—a dataset of global glacier outlines: Version 6.0: *Technical Report Global Land Ice Measurements from Space* (Boulder, CO: Digital Media) (<https://doi.org/10.7265/N5-RGI-60>)
- Sabeerali C T, Rao S A, Dhakate A R, Salunke K and Goswami B N 2015 Why ensemble mean projection of south Asian monsoon rainfall by CMIP5 models is not reliable? *Clim. Dyn.* **45** 161–74

- Schneider U, Becker A, Finger P, Meyer-Christoffer A, Rudolf B and Ziese M 2011 GPCC full data reanalysis Version 6.0 at 0.5°: monthly land-surface precipitation from rain-gauges built on GTS-based and historic data
- Shahid S 2011 Trends in extreme rainfall events of Bangladesh *Theor. Appl. Climatol.* **104** 489–99
- Srivastava A K and DelSole T 2014 Robust forced response in south Asian summer monsoon in a future climate *J. Clim.* **27** 7849–60
- Stackhouse P W Jr, Gupta S K, Cox S J, Mikovitz C, Zhang T and Hinkelman L M 2011 The NASA/GEWEX surface radiation budget release 3.0: 24.5-year dataset *GEWEX News* **21** 10–12 (available at: www.gewex.org/resources/gewex-news/)
- Taylor K E, Stouffer R J and Meehl G A 2012 An overview of CMIP5 and the experiment design *Bull. Am. Meteorol. Soc.* **93** 485–98
- Uhe P F, Mitchell D M, Bates P D, Sampson C C, Smith A M and Islam A S 2019 Enhanced flood risk with 1.5 °C global warming in the Ganges–Brahmaputra–Meghna basin *Environ. Res. Lett.* **14** 074031
- Vetter T, Huang S, Aich V, Yang T, Wang X, Krysanova V and Hattermann F 2015 Multi-model climate impact assessment and intercomparison for three large-scale river basins on three continents *Earth Syst. Dyn.* **6** 17–43
- Vinke K et al 2017 Climatic risks and impacts in South Asia: extremes of water scarcity and excess *Reg. Environ. Change* **17** 1569–83
- Wang B, Chunhan J and Jian L 2020 Understanding future change of global monsoons projected by CMIP6 models *J. Clim.* **33** 6471–89
- Weedon G P, Balsamo G, Bellouin N, Gomes S, Best M J and Viterbo P 2014 The WFDEI meteorological forcing data set: WATCH forcing data methodology applied to ERA-interim reanalysis data *Water Resour. Res.* **50** 7505–14
- Wortmann M, Bolch T, Menz C, Tong J and Krysanova V 2018 Comparison and correction of high-mountain precipitation data based on glacio-hydrological modeling in the tarim river headwaters (High Asia) *J. Hydrometeorol.* **19** 777–801
- Xin X, Wu T, Zhang J, Yao J and Fang Y 2020 Comparison of CMIP6 and CMIP5 simulations of precipitation in China and the East Asian summer monsoon *Int. J. Climatol.* **40** 6423–40